 doi:10.20944/preprints202210.0339.v1

Article

A Smartphone-based Low-Cost Inverted Laser Fluorescence Microscope for Disease Diagnosis

Omar Ormachea [1,*], Alex Villazón [2], Patricia Rodriguez [3] and Mirko Zimic [4]

[1] Centro de Investigaciones Opticas y Energías (CIOE), Universidad Privada Boliviana (UPB), Cochabamba, Bolivia; oormachea@upb.edu
[2] Centro de Investigaciones en Nuevas Tecnologías Informáticas (CINTI), Universidad Privada Boliviana (UPB), Cochabamba, Bolivia; avillazon@upb.edu
[3] Instituto de Investigaciones Biomédicas (IIBISMED), Facultad de Medicina, Universidad Mayor de San Simón (UMSS), Cochabamba, Bolivia; p.rodriguez@umss.edu.bo
[4] Laboratorio de Bioinformática, Biología Molecular y Desarrollos Tecnológicos, Facultad de Ciencias y Filosofía, Universidad Peruana Cayetano Heredia (UPCH), Lima, Perú; mirko.zimic@upch.pe
* Correspondence: oormachea@upb.edu

Abstract: Fluorescence microscopy is an important tool for disease diagnosis, often requiring costly optical components, such as fluorescence filter cubes and high-power light sources. Due to its high cost, conventional fluorescence microscopy cannot be fully exploited in low-income settings. Smartphone-based fluorescence microscopy becomes an interesting low-cost alternative, but raises challenges in the optical system. We present the development of a low-cost inverted laser fluorescence microscope, that uses a smartphone to visualize the fluorescence image of biological samples. Our fluorescence microscope uses a laser-based simplified optical filter system, that provides analog optical filtering capabilities of a fluorescence filter cube. Firstly, we validated our inverted optical filtering by visualizing microbeads labeled with three different fluorescent compounds or fluorophores, commonly used for disease diagnosis. Secondly, we validated the disease diagnosis capabilities, by comparing the results of our device with those of a commercial fluorescence microscope. We successfully detected and visualized Trypanosoma cruzi parasites, responsible of the Chagas infectious disease, and the presence of Antineutrophil cytoplasmic antibodies of the ANCA non-communicable autoimmune disease. The samples were labeled with the fluorescein isothiocyanate (FITC) fluorophore, one of the most commonly used for disease diagnosis. Our device provides a 400 X magnification and is at least two orders magnitude cheaper than conventional commercial fluorescence microscopes.

Keywords: low-cost fluorescence microscopy; smartphone microscopy; 3D-printed devices; laser-based microscopy

1. Introduction

Fluorescence microscopy and the use of fluorescent molecules (i.e., fluorophores) in biology is a powerful tool in healthcare [25]. Although commercial fluorescent microscopes are widely available, their high costs (mainly due to sophisticated optics for light filtering) strongly limit their use in low-income settings. Moreover, operating these microscopes requires trained personnel, who know how to label the samples with fluorophores, operate the microscope, choose the correct wavelength, and interpret the fluorescence images through visualization.

Smartphone microscopy [26] has become an interesting alternative, enabling more compact, affordable, and flexible solutions compared to conventional microscopy. However, many microscopic techniques in the area of disease diagnosis require a minimum optical magnification of 400X, often not reached by this type of low-cost microscopes.

Low-cost fluorescence microscopy [27–34], raises several challenges, mainly in the optical system, that requires special filtering of the light sources (e.g., LEDs or lasers) used

Preprints (www.preprints.org) | NOT PEER-REVIEWED | Posted: 21 October 2022 doi:10.20944/preprints202210.0339.v1

to excite the fluorophores, while keeping the filtering system affordable, notably avoiding the use costly fluorescence microscope cubes from conventional fluorescence microscopy (based on dichroic mirrors and special filters).

Fluorescence microscopy is an effective procedure for the diagnosis of many infectious and non-communicable diseases [25]. It is often the only way to make a diagnosis. Many microorganisms (e.g., parasites, bacteria) can be specifically detected and identified through fluorescence labeling. The use of fluorochrome-labeled antibodies facilitates this identification, increasing detection sensitivity and improving specificity with respect to white light optical microscopy.

For disease diagnosis, low-cost fluorescence microscopy can be seen as an interesting alternative for low-income countries, where several endemic diseases (e.g. Chagas and Tuberculosis) affect millions of people, and are also spreading in non-endemic areas, such as Europe, USA, Canada and Japan, mainly through migration [35,36]. Also, several non-communicable diseases, e.g., autoantibodies and autoimmune diseases [25], are not detected on-time due to the lack of fluorescence microscopes in low-income settings.

In general, disease diagnosis requires the detection and identification of microorganisms (e.g., parasites, bacteria, or cells), through fluorescence labeling. In [33] a low-cost fluorescence microscope is used to detect Mycobaterium tuberculosis, using auramine fluorophore [37], which reduces the required 1000X magnification for conventional non-fluorescence techniques to only 400X. Unfortunately, because of the complexity of the optical filtering system, other low-cost fluorescence microscopes [27–32,34], do not reach required magnification for diagnosis of 400X, and are either a proof-of-concept (to identify fluorescent particles) or are limited to the visualization of cells, but cannot be used for diagnosis.

In this article, we present a smartphone-based low-cost inverted fluorescence microscope, which has a simplified optical filter system, can reach at least a 400X of magnification, and can be used for disease diagnosis (infectious and non-communicable diseases). Our hypothesis is that it is possible to replace the costly optical fluorescence filter cubes with a simplified filter based on a low-cost laser and a cheap barrier filter. Our microscope uses an inverted optical scheme to avoid the need of a dichroic mirror and two special filters (excitation and barrier filters), thus allowing both the laser excitation signal and the fluorescence signal (from the labeled sample) to reach the single barrier filter, which lets only the fluorescence signal reach the smartphone's camera.

Our proposed device is compatible with all diagnostic kits that use fluorescein isothiocyanate (FITC) as labeling dye [38,39]. FITC is one of the more commonly used fluorophores for diagnosis, due to its high absorption, excellent fluorescence quantum yield, affordable cost, and good water solubility [40].

Instead of using the standard 488 nm wavelength for the excitation signal, used by conventional fluorescence microscope (which is closer to the maximum excitation absorption peak of the FITC fluorophore at 495 nm), our inverted microscope uses a low-cost 405 nm laser source resulting in a much lower absorption. Our hypothesis is that, since we use a focalized high-intensity laser source, this will compensate the low-level absorption of FITC, thus obtaining fluorescence images similar to those of a conventional fluorescence microscope.

The validation of our proposed device was done in two ways:

- We validate the proposed low-cost laser-based simplified filtering system, by using microbeads labeled with three fluorophores commonly used for disease diagnosis (i.e., FITC, PE and PE-Cy5).
- We validate the diagnosis capability of our device, by using biological samples of two diseases (one infectious and one non-communicative), and comparing the obtained results with those of a conventional fluorescence microscope. The samples were labeled with FITC fluorophore.

For the diagnosis of infectious disease, we chose Chagas, an endemic disease that affects millions of people, mainly in Latin America, that is caused by the protozoan parasite

 doi:10.20944/preprints202210.0339.v1

Trypanosoma cruzi (T. cruzi) and is transmitted in the endemic areas during a bite of a hematophagous insect belonging to the Triatominiae family. In non-endemic areas, the transmission occurs mainly by blood transfusion, organ transplant from infected people or vertical transmission from mother to child [35]. The diagnosis of Chagas by immunofluorescence requires the visualization of fixed forms of T. cruzi apimastigotes, indirectly labeled with a fluorophore (e.g., FITC or Alexa Fluor 488). This visualization of the fluorescent T. cruzi parasite requires a magnification of at least 400X.

For the diagnosis of non-communicable disease, we chose ANCA test. Anti-neutrophil cytoplasm antibodies (ANCA) are autoantibodies that target mainly antigens present in cytoplasmic granules of neutrophils an autoimmune disease affecting small blood vessels in the body [41]. The diagnosis of this disease is done by observing granules on fixed neutrophils after indirect marking with FITC fluorophore.

2. Materials and Methods

In this section we describe our proposed simplified optical filtering system (avoiding sophisticated optical filtering as those of conventional fluorescence microscopes), the 3D-printed structure of our inverted microscope, and the use of a low-cost laser for sample excitation at 405 nm for FITC labeling.

2.1. Simplification of the fluorescence filtering system

To avoid high costs of special filter cubes used by conventional fluorescence microscopes, we propose a simplified filtering system, based on a longpass filter and a laser signal with narrow spectral width. First, we describe how conventional fluorescence filter cubes work, which includes a barrier filter, a dichroic mirror, and an excitation filter. Then, we describe our simplified system, which includes a longpass filter and replaces the excitation filter and the dichroic mirror with a laser module.

2.1.1. Operation of a conventional fluorescence filter cube

Fluorescence microscopy uses, for fluorochrome excitation, different sources of light, e.g., mercury vapor lamps, halogen lamps, and LED. All these light sources produce white light, thus requiring a fluorescence filter cube, consisting of two types of filters (excitation and barrier filter), and a dichroic mirror (see Fig.1(a)). Fluorescence filter cubes can either have a longpass or a bandpass barrier filter[1], depending on wavelength range of the fluorescence to filter. The excitation filter is used to separate a narrow part of the white light source (see parallel yellow arrows in Fig. 1(a)), that becomes the excitation signal for the fluorophore. The wavelength of the excitation signal must be close to the fluorophore's absorption peak. In order to let the excitation signal to reach the sample, a dichroic mirror (placed at 45°) reflects the excitation signal to the sample (see downwards blue arrow in Fig. 1(a)). It then generates fluorescence in a different wavelength. Both the excitation and fluorescence signals are sent to the microscope's ocular (see the upwards red arrow in Fig. 1(a)), thus requiring a barrier filter to block excitation signal, and let only the fluorescence signal to pass.

[1] https://www.microscope.healthcare.nikon.com/products/accessories/fluorescent-filter-cubes/

Preprints (www.preprints.org) | NOT PEER-REVIEWED | Posted: 21 October 2022 doi:10.20944/preprints202210.0339.v1

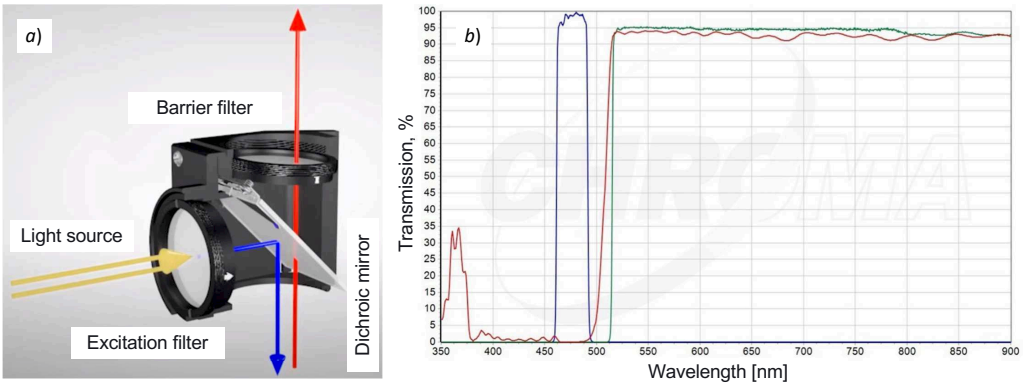

Figure 1. Filtering system of a conventional fluorescence microscope. (**a**) Operation of a fluorescence filter cube and (**b**) Transmission spectra of the optical components of a longpass filter cube for FITC fluorophore.

The Fig.1(b) shows the transmission spectra of the optical components of a longpass filter cuber for FITC fluorophore (excitation filter 480/30, dichroic mirror 505, barrier filter 515, and filter diameter 25 mm). We can observe a reduced spectral bandwidth excitation signal of around 30 nm, generated by the excitation filter (see the blue curve between 450 nm and 500 nm in The Fig.1(b)). The red curve shows the spectral behavior of the dichroic mirror, and the green curve shows the longpass filtering of the excitation signal, i.e., it makes the bypass filter completely transparent to the fluorescence signal.

2.1.2. Using low-cost laser source to increase the optical excitation signal

To reduce the cost of sophisticated optics for light filtering of a fluorescence filter cube, we need to reproduce a similar longpass excitation signal filtering as described before. The key idea of our approach is to replace the combination of a) the white light excitation source, b) the excitation filter, and c) the dichroic mirror, by a single low-cost laser source. The principle is that the laser has a very narrow spectral bandwidth (of around 5 nm), thus avoiding the need of the excitation filter (which was used to reduce the spectral bandwidth of the white light source). Furthermore, the dichroic mirror is not needed anymore, because the sample is directly excited by the laser beam. In addition, the intensity of the excitation laser signal is orders of magnitude higher than the any white light source, thus increasing the fluorescence signal significantly. Finally, in our approach the use of a longpass barrier filter remains the same as in the conventional fluorescence filter cube, because we need to block the excitation signal while letting the fluorescence signal pass through.

Fig.2(a) shows the continuous focusable low-cost CW laser module we use, which has the following characteristics: Wavelength = 405 nm, Voltage = 12VDC, Current = 280 mA, Optical power = 600 mW, PWM = 20 kHz-50 kHz / 3.3VDC-12VDC, Radiator size = 3 $\times$6 cm, and Weight = 116 g.

Preprints (www.preprints.org) | NOT PEER-REVIEWED | Posted: 21 October 2022 doi:10.20944/preprints202210.0339.v1

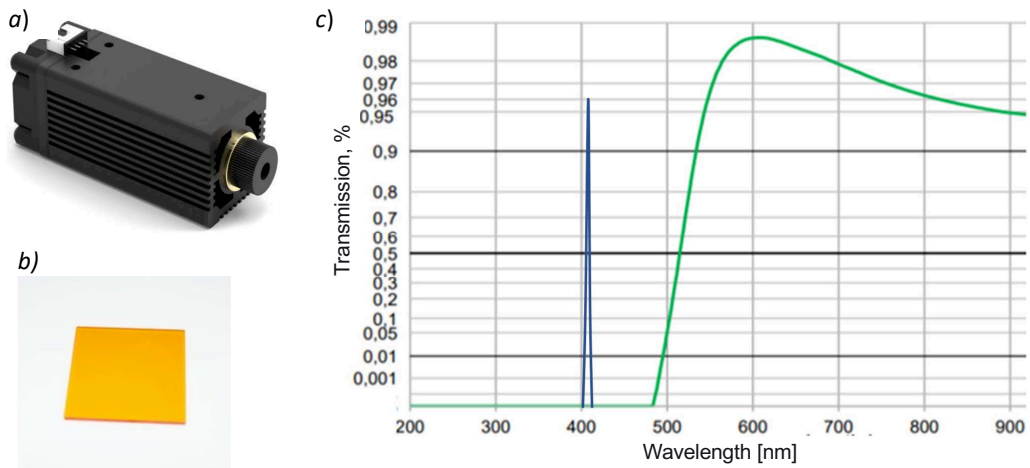

Figure 2. (**a**) The 405 nm laser module, (**b**) the longpass OG515 filter, and (**c**) the transmission spectra of the OG515 filter in green, and in blue the emission peak of the 405 nm laser module.

Fig. 2(b) shows the standard longpass OG515 filter used in our simplified filter system. The size of this filter is 25.4 ×25.4 ×3 mm and its transmission spectra is shown in Fig. 2(c), which was obtained using SCHOTT's Interactive Filter Diagram[2]. We can observe that the longpass OG515 filter completely absorbs the excitation signal at 405 nm. This confirms that our simplified laser-based filtering system is analog to the one of a conventional fluorescence filter cube shown in Fig. 1(c), but the cost of the proposed system is at least one order of magnitude cheaper.

2.2. The design and structure of the inverted microscope

Once the simplified low-cost laser-based longpass filter system was defined, we needed to find the most adapted structure, both to hold the filtering system, and to allow direct sample excitation with the laser beam (to avoid the need of a dichroic mirror). We found that an inverted microscope scheme fulfilled these requirements. Therefore, we used a baseline the structure of a non-fluorescence inverted smartphone-based microscope from [42], that was used for tuberculosis diagnosis. We adapted the structure to include the laser module on top of the sample holder, to increase the magnification (from 100X to at least 400X), to integrate the longpass filter within the optical scheme, and to add X-Y-Z stage of samples.

Our proposed inverted microscope consists of a continuous focusable 405 nm laser, a long pass OG515 filter, a high bright white LED, an optical ocular, an objective lens, a mechanical stage for biological microscope, and a 3D-printed structure, which includes a a sample positioning system (X-Y and Z), and a smartphone holder (see Fig. 3). All the optical and mechanical components are inexpensive and can be easily found.

The optical structure and operating principle of the inverted microscope and our simplified filtering system is shown in Fig. 4(a). Once the sample is positioned, the laser beam directly excites the sample from the top. Both the excitation signal (blue dashed arrow) and the flourescence signal (green dashed arrow) crosses the objective lens, and are reflected by a first conventional mirror positioned at 45°. Both signals reach the longpass OG515 filter, and the excitation signal is blocked. The filter lets the fluorescence signal to reach the second mirror and cross the ocular, where the resulting image is amplified. The camera of the smartphone is positioned on the hole of the smartphone holder (see Fig. 4(b)). The smartphone therefore captures the image with the fluorescence emitted by the sample labeled with a fluorophore, and the operator can directly visualize it and perform the diagnosis.

[2] https://www.schott.com/en-dk/interactive-filter-diagram

Preprints (www.preprints.org) | NOT PEER-REVIEWED | Posted: 21 October 2022 doi:10.20944/preprints202210.0339.v1

Note that the LED white light is not used for sample excitation, but only for initial sample illumination, e.g., for positioning the sample and help with the focusing through the X-Y and Z positioning system. Thus, the operator must first turn ON the white LED light, focus the image and only then turns ON the laser module.

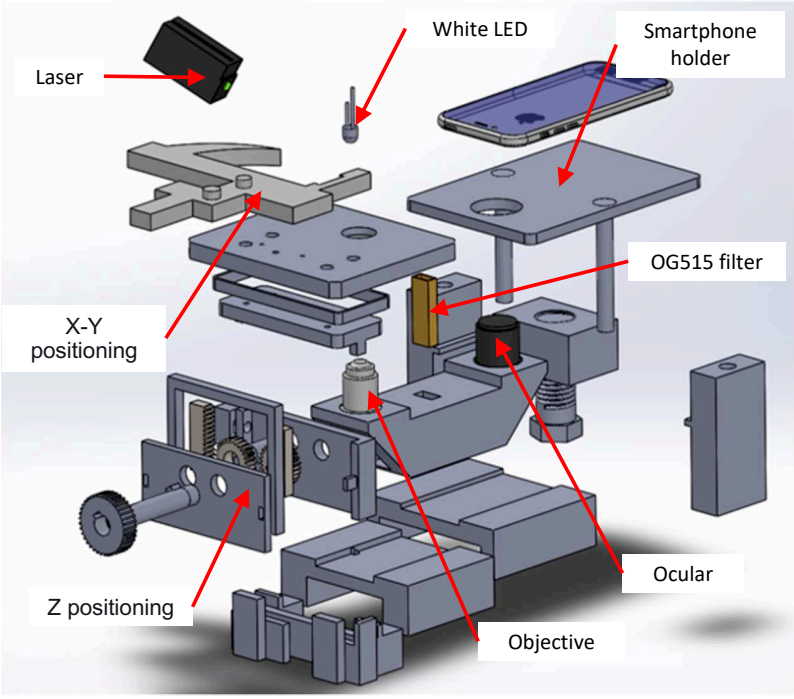

Figure 3. Block diagram of the 3D-printed laser fluorescence inverted microscope.

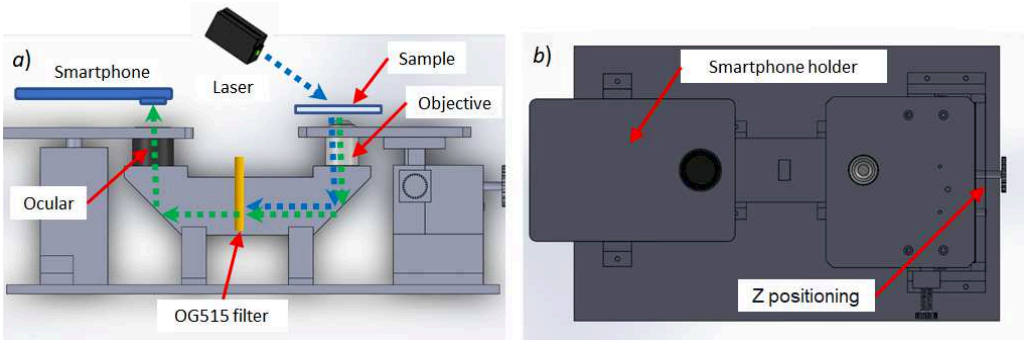

Figure 4. 3D-printed designed scheme. (**a**) Side view design showing the simplified longpass filtering system, and (**b**) Top view design, where the smartphone is positioned and the Z-positioning gear.

Our positioning system includes a conventional X-Y stage for microscopes that was adapted to the 3D-printed structure. For the Z positioning, a 3D-printed system of gears was designed to allow coarse grain vertical movements of the piece where the objective lens is placed. Once the Z coarse adjustment is made through the 3D-printed gear, we used the objective lens's screw for the fine grain focusing. This allows the microscope operator to feel almost no difference compared to a conventional microscope, hence also reducing the costs of using a high-precision Z stage.

For an adequate magnification for disease diagnosis, that is typically used in fluorescence microscopy, we use an ocular objective and an objective lens with 10X and 40X magnification, respectively (see Fig.5(a) and Fig.5(b)). Both objectives are assembled in the 3D-printed mechanical structure. The total magnification of our inverted microscope is of 400X.

Preprints (www.preprints.org) | NOT PEER-REVIEWED | Posted: 21 October 2022 doi:10.20944/preprints202210.0339.v1

Figure 5. Optical and opto-mechanical components. (**a**) Optical ocular ZEISS MF-projektiv K 10X; (**b**) Achromatic objective lens OMAX with 40X of magnification, and (**c**) OMAX X-Y microscope stage.

For the handling and positioning of the samples in the microscope, a conventional X-Y stage was integrated in the 3D-printed structure. The Fig.5(c) shows the X-Y mechanical stage for biological microscope.

2.3. Proposed laser excitation for FITC labeling

FITC is a synthetic organic dye that ease the bio-conjugation with proteins (immunoglobulins) without interfering with their biological function. For several serological tests based on fluorescence labeling, FITC in one of the most commonly used fluorophores [38,39], due to its high absorption, excellent fluorescence quantum yield, affordable cost, and good water solubility [40].

FITC has an excitation absorption peak close to 495 nm [43–45]. For conventional fluorescence microscopy, the excitation is provided by a fluorescence filter cube 480/30 (where 480 nm is the peak of transmission with 30 nm of bandwidth). FITC is an important fluorophore not only for fluorescence microscopy, but also for confocal microscopy, and flow cytometry [46,47], where the main emission wavelength of the light sources (fluorescence filter cube 480/30 and argon ion laser) are also close the 495 nm absorption peak (480 nm and 488 nm), respectively.

For our low-cost inverted microscope, we propose the use of the laser excitation at 405 nm, instead of costly high-power light sources (e.g., mercury or halogen lamps) combined with a fluorescence filter cube with a closer wavelength to the FITC excitation peak at 495 nm.

Fig. 6 shows the absorbance and emission spectra of FITC fluorophore obtained with the DB Spectrum Viewer[3], with two different excitation wavelengths. Fig. 6(a) shows the maximum excitation wavelength for FITC at 495 nm, that results in the highest fluorophore absorption band (the dotted light blue curve). Therefore, the closest the wavelength the excitation source is to the peak of the dotted curve, the highest will be the absorption, and consequently the highest will be the fluorescence emission.

Since we propose to use a low-cost laser with its excitation wavelength at 405 nm, we can observe in Fig. 6(b) that the absorption of FITC is rather low, and consequently the lower will be the fluorescence emission.

However, since we are using a focalized laser source with a very narrow spectral bandwidth and a large number of emitted photons, this compensates the low-level absorption of FITC. Our hypothesis is therefore, that the use of the low-cost laser source, even though it is not at the peak of the FITC absorption band, we will be able to obtain a fluorescence value of sufficient intensity to clearly observe that signal.

In the next section, we show how this hypothesis was validated by testing microbeads labeled with 3 different fluorophores, and later with real biological samples.

[3] https://www.bdbiosciences.com/en-us/resources/bd-spectrum-viewer

Preprints (www.preprints.org) | NOT PEER-REVIEWED | Posted: 21 October 2022 doi:10.20944/preprints202210.0339.v1

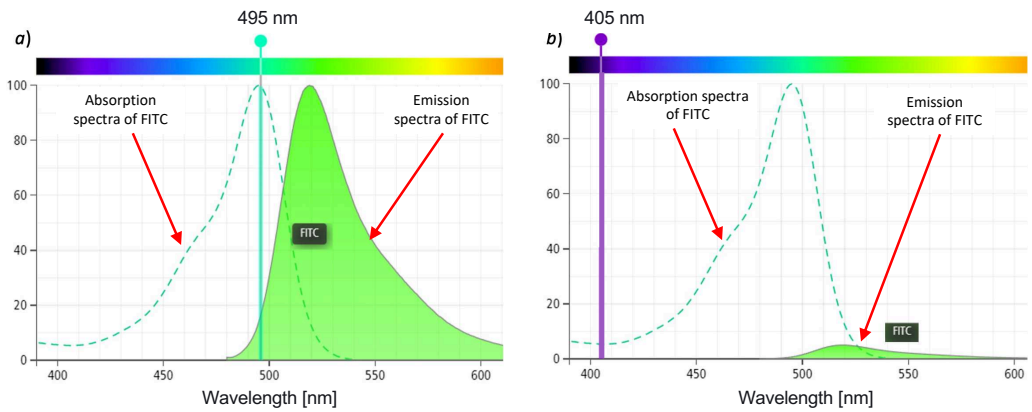

Figure 6. Absorbance and emission spectra of FITC fluorophore (**a**) Excitation at 495 nm, and (**b**) Excitation at 405 nm.

3. Results

In this section, we present the main results, which include the fully functional inverted microscope, the smartphone's App to process and visualize the images, the validation of the proposed filtering system with three different fluorophores, and the fluorescence images obtained with real Chagas parasites and ANCA granules in neutrophil cytoplasm, labeled with FITC with the 400X magnification. We also include the total cost of the proposed inverted microscope.

3.1. Assembling of a 3D-printed structure

The proposed device was 3D-printed in a Flashforge Creator Pro 3D printer with a precision of 0.1 mm and the use of a PLA filament (as shown in Fig.7). The piece containing all the optical elements of the filtering system (objective lens, OG515 filter, ocular, and mirrors) were assembled in a compact box, printed with black PLA filament and with higher density, to minimize the interference of the external light.

The device consists of an inverted microscope structure and a smartphone. The smartphone is positioned on the structure's 'smartphone holder' (with the turned-on camera). The sample slide is positioned in the 'sample holder', and the X-Y stage moves the slide to the correct position. The X-Y positioning system is a conventional X-Y microscope stage clip, allowing the operator to handle samples in a standard way. The images can be observed directly on the smartphone's screen. The user only needs to turn ON the white LED and adjust the focus for the visualization of the magnified image. Then, just turn ON the laser module and turn OFF the LED to obtain a fluorescence image of the samples.

Our developed microscope is a small ($30 \times 35 \times 14$ cm), robust, light-weight, and portable, requiring only electric power to operate the laser module.

Preprints (www.preprints.org) | NOT PEER-REVIEWED | Posted: 21 October 2022 doi:10.20944/preprints202210.0339.v1

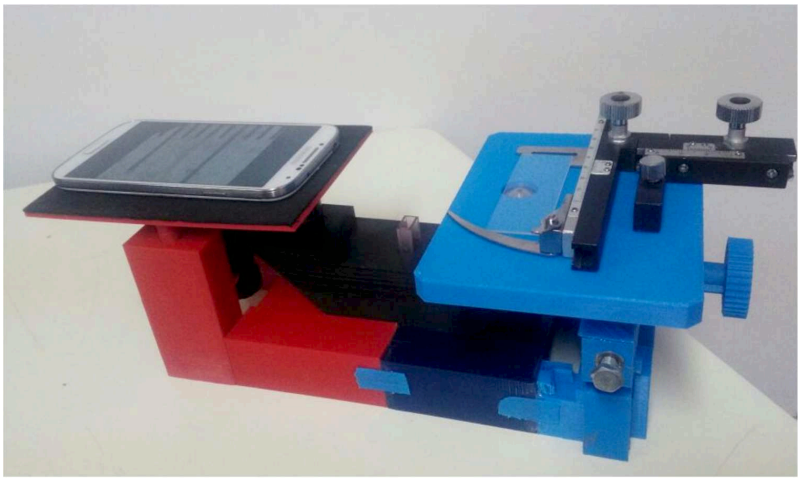

Figure 7. The 3D-printed structure of our smartphone-based inverted laser fluorescence microscope.

3.2. Smartphone processing and optical magnification of the microscope

We developed an Android App (MicroscopeUPB) to capture, process, and store the images and videos generated by the microscope. The data is organized using an embedded database. The App allows the user to control the autofocus and lock it according to the user's requirement. Since the smartphone's camera captures the 400X magnified image directly from our microscope's ocular lens (placed in the hole of the smartphone's holder), the image displayed on the screen is shown as a circle that does not cover the full screen, and therefore is not very practical. The App, therefore, applies an automatic adjustment to the obtained image, so as to fit the ocular lens's circle in the entire screen. This is done cropping the circle and applying a 1.5X magnification with digital zoom.

Fig.8(a) shows the inverted fluorescence microscope and the App in operation; Fig.8(b) shows the main screen with the options to capture the images and view previously stored experiment data; and Fig.8(c) shows the capture options for different experiments.

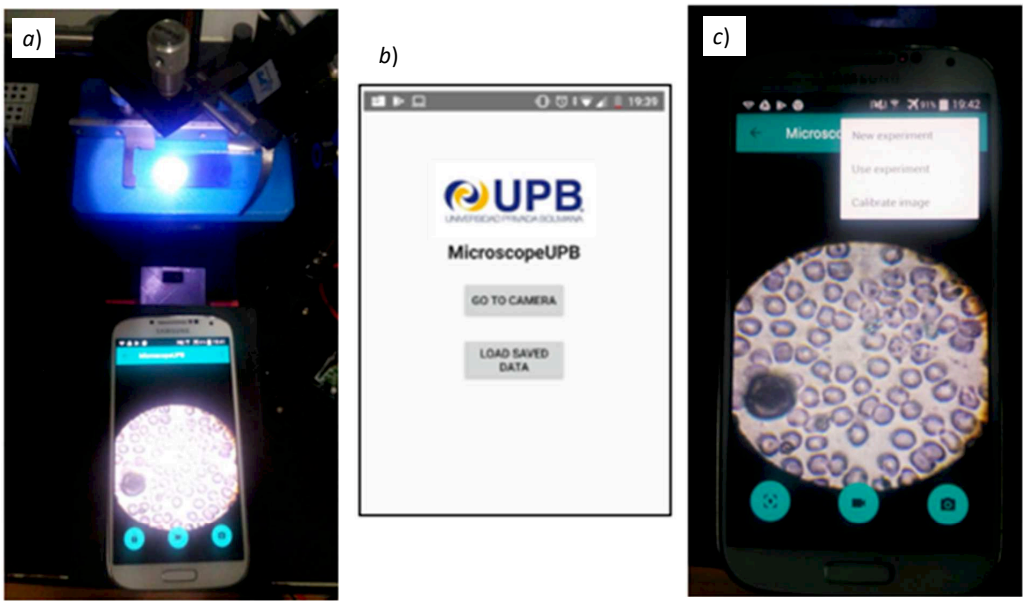

Figure 8. The Android App "MicroscopeUPB" for image capture and processing in operation. (**a**) Calibration of positioning; (**b**) Main screen of the App; and (**c**) Capture options for experiments.

To validate the magnification of the device, we used a Stage Micrometer Microscope Calibration Slider. Fig.9 shows the lines of the 10 µm calibration slider (on the right side), compared with the image captured with our microscope showing T. cruzi parasites (on

Preprints (www.preprints.org) | NOT PEER-REVIEWED | Posted: 21 October 2022 doi:10.20944/preprints202210.0339.v1

the left side). This comparison confirms that our device has at least a 400X magnification, which is similar to the one obtained with conventional microscopes. Note that the image was captured without using the digital zoom of the smartphone camera and only the white LED light was used to capture the image.

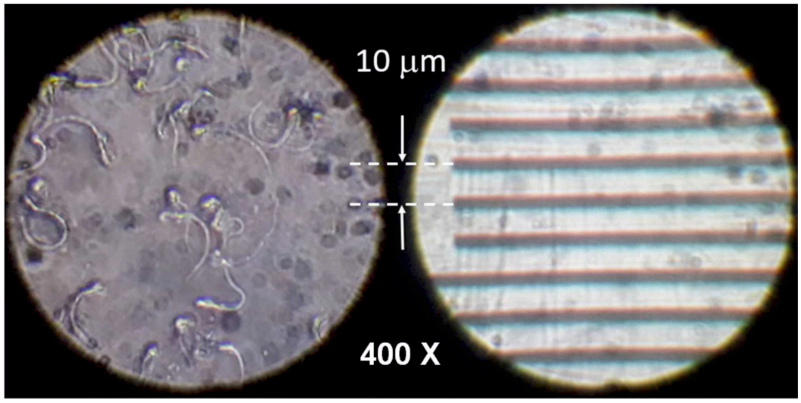

Figure 9. Effective magnification of the developed inverted microscope.

3.3. Validation of the simplified filtering system

Our initial hypothesis was that we could use a laser excitation source at 405 nm instead of a standard wavelength of 488 nm, which is commonly used for a large variety of fluorophores in diagnostic techniques with fluorescence microscopy. Fig. 10(a) shows the absorption and emission spectra for the FITC, PE and PE-Cy5 fluorophores, under an excitation at 488 nm. We can clearly see that with that wavelength all three fluorophores have high absorption curves and are close to their absorption peaks. Again, these peaks can be obtaining by using different types of light sources, but different and costly fluorescence filter cubes are needed.

To validate our hypothesis, we need to show that using a laser with a different excitation signal (at 405 nm), thanks to the intense radiation and our simplified filter system, we are able to observe samples labeled with those fluorophores. For this, we use calibration microbeads that are normally applied for verification and normalization of fluorescence intensities in flow cytometers. Fig.10(b) shows an example[4] of such microbeads, which can be labeled with the desired fluorophore upon request. Typical dimensions of these microbeads are in the range of 2 µm to 6 µm, which require a magnification of 400X to be observed properly.

[4] https://www.applied-microspheres.com/cyto-cal-multifluor-fluorescence/

Preprints (www.preprints.org) | NOT PEER-REVIEWED | Posted: 21 October 2022 doi:10.20944/preprints202210.0339.v1

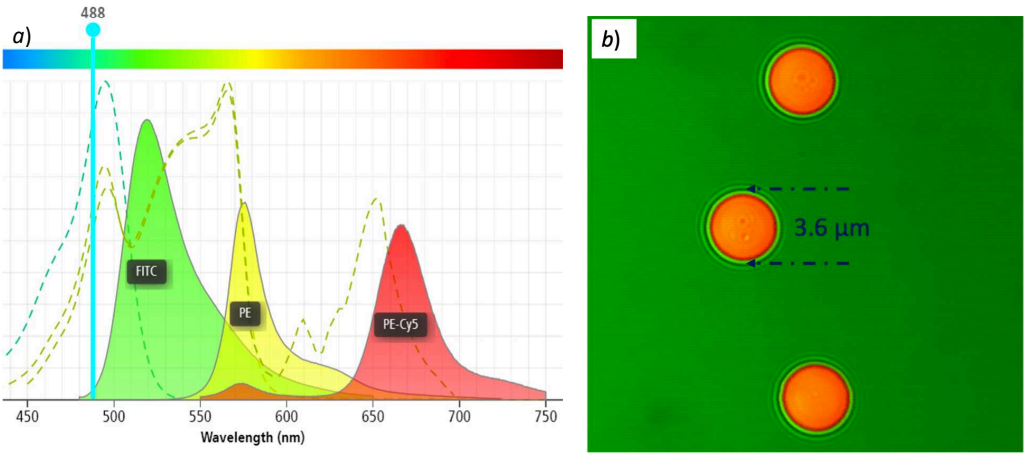

Figure 10. (**a**) Absorption and emission spectra of FITC, PE and PE-Cy5 fluorophores, under 488 nm excitation; (**b**) Sample calibration microbeads for flow-cytometry.

We used our inverted fluorescence microscope to experimentally observe the fluorescence of microbeads labeled with FITC, PE and PE-Cy5 fluorophores. The microbeads are present in a liquid solution that is put in a glass slide that is positioned in the X-Y stage, and the laser is turned ON. After correct focusing and positioning, we were able to observe all three fluorophores. Fig.11(a) and Fig.11(b) show the fluorescence images obtained of the 3.6 µm microbeads labeled with ① FITC, ② PE, and, ③ PECy5. As shown in Fig.11(c), the emission peaks of these spheres, with a 405 nm excitation source, correspond to 519 nm (green color), 576 nm (yellow color) and 665.8 nm (red color), which are all in the visible part of the electromagnetic spectrum. Thanks to the intensity of the laser we use, even though the emission curves are rather low, the obtained fluorescence images are visible with our device. This confirms that our simplified filter system works correctly, even with a non-optimal emission source.

Preprints (www.preprints.org) | NOT PEER-REVIEWED | Posted: 21 October 2022 doi:10.20944/preprints202210.0339.v1

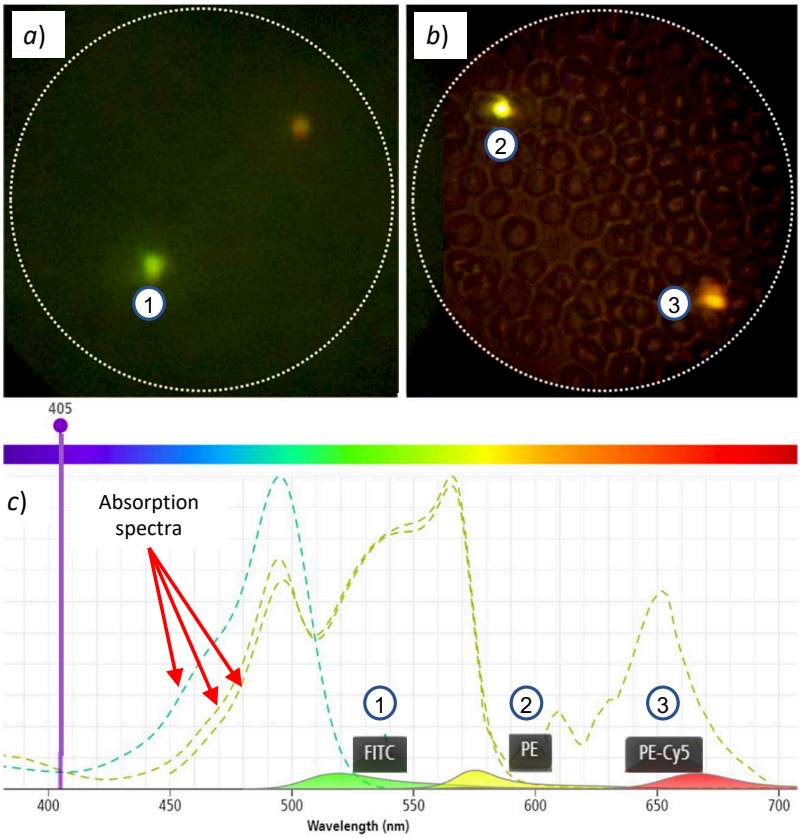

Figure 11. (**a**) Captured image of fluorescence of microbead labeled with FITC fluorophore; (**b**) Fluorescence of microbeads labeled with PE and PE-Cy5 fluorophores; and (**c**) absobption/emission spectra of microbeads under 405 nm laser excitation.

3.4. Validation of our approach with real biological samples labeled with FITC

We validated our inverted fluorescence microscope by capturing images of real biological samples and comparing them with those obtained with a commercial conventional inverted microscope. For the validation we chose samples of T. cruzi parasites and granules of neutrophil cytoplasm, both labeled with FITC fluorophore.

3.4.1. Validation with Chagas infectious disease

The epimastigotes forms of T. cruzi parasites were fixed on glass plates were indirectly labeled using anti-human immunoglobulin IgG+IgM-FITC conjugate (Vircell, Chagas IFA IgG-IgM Kit Ref. PCHAG). The labeling process was carried out following the kit supplier's instructions. For T. cruzi staining, we used pooled human serum control from chronic chagasic and non-chagasic patients with 1:40 - 1:80 dilutions. Briefly, after sera dilution, 20 −25 µL of each sample was placed in each of the slide wells and incubated for 30 ± 5 min at 37 °C. After two 5 min washes, they were incubated for 30 min with 25 µL/well with the respective FITC-labeled conjugate in Evan's blue. After a new wash, the slides were mounted with buffered glycerin under coverslips for microscopic observation.

To compare the images obtained with our device, we used a commercial conventional fluorescence Motic BA410E microscope[5] with a magnification of 400 X, using Eyepieces130N-WF 10X/22 and Objective EC-H Plan Achromats 40X/0.65. We used the same samples of T. cruzi parasites labeled with FITC fluorophore with both devices.

Fig.12(a) shows the image captured with our device, whereas Fig.12(b) shows the images captured by the commercial microscope. We can clearly see that our microscope is capable to identifying the T. cruzi parasites. We can observe that the commercial mi-

[5] https://moticeurope.com/en/microscope/serie/ba410e

Preprints (www.preprints.org) | NOT PEER-REVIEWED | Posted: 21 October 2022 doi:10.20944/preprints202210.0339.v1

croscope has more intensity, which is due to the use of the optimal excitation signal. The images obtained with our device are slightly less intense, because the use of the laser degrades rapidly the fluorophore due to the intense focalized laser beam. We also can see that the image obtained with our device shows bigger T. cruzi parasites (even though both microscopes have 400X magnification). This is due to a digital zoom made by our smartphone App to fit the ocular lens output on the screen.

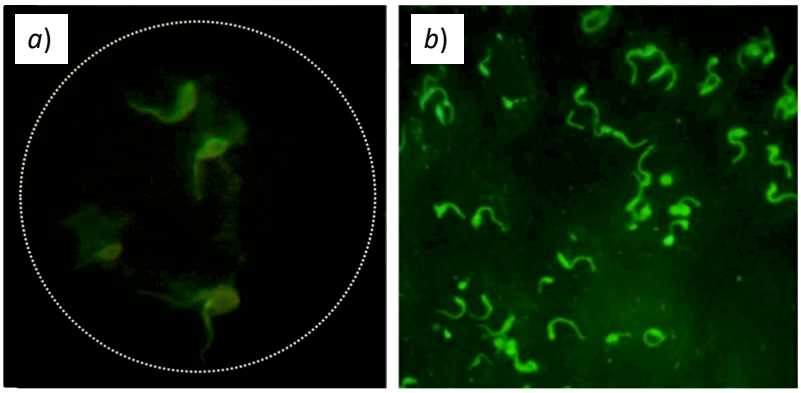

Figure 12. Fluorescence images of T. cruzi parasites labeled with FITC fluorophore, obtained with (**a**) our inverted fluorescence microscope; (**b**) a commercial Motic BA410E fluorescence microscope.

3.4.2. Validation with ANCA non-communicable disease

ANCA is a type of autoimmune disease that causes vasculitis. ANCA stands for Anti-Neutrophilic Cytoplasmic Autoantibody. Our device was also tested by visualizing neutrophils indirectly labeled with FITC labeled anti-human IgG conjugate to find auto-antibodies against proteins of the cytoplasmic granules (Inova Diagnostics, NOVA Lite© ANCA Kit, Ref. 708290). For the labeling of neutrophils, undiluted ANCA positive and negative control from the kit were used. As for the T. cruzi sample preparation, we followed the kit supplier's instruction, and put the samples in the slides for observation. Fig.13(a) shows the image captured with our device, whereas Fig.13(b) shows the images captured by the commercial microscope.

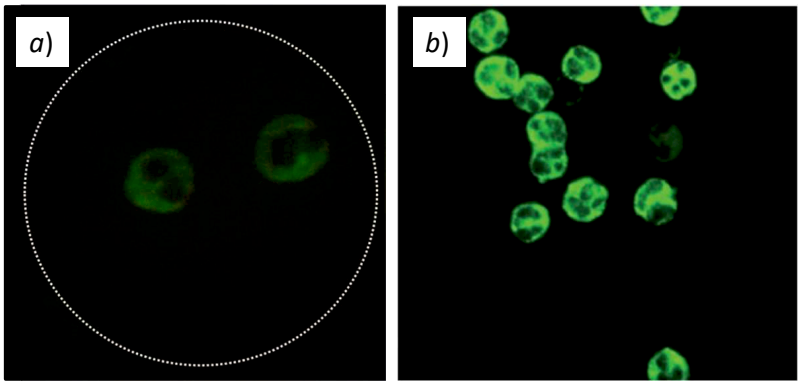

Figure 13. Fluorescence images of granules in neutrophil cytoplasm labeled with FITC fluorophore obtained with (**a**) our inverted fluorescence microscope; (**b**) a commercial Motic BA410E fluorescence microscope.

Overall, we can confirm that our low-cost inverted fluorescence microscope is capable of capturing similar images from real biological samples labeled with FITC, and therefore can be used for disease diagnostic and biomedical applications.

Preprints (www.preprints.org) | NOT PEER-REVIEWED | Posted: 21 October 2022 doi:10.20944/preprints202210.0339.v1

3.5. Cost of the proposed low-cost inverted fluorescence microscope

The total cost of our proposed low-cost fluorescence microscope is around 240 $, which makes it affordable for low-income settings. Table 1 shows the list of components that are required to build the device, along with their cost. Note that the cost of the two components of our simplified longpass filtering system (i.e., the laser module and the OG515 long pass filter), do not exceed 130 $, which is largely less expensive than a commercial fluorescence filter cube, which price is of around 1000 $.

Table 1. Breakdown costs of our low-cost laser inverted fluorescence microscope.

Component Used	Model / Specification	Estimated cost (USD)
X-Y Stage	OMAX X-Y Mechanical Stage for Biological Microscope	20
Ocular Lens	ZEISS MF-projektiv K 10X	20
Objective Lens	OMAX Achromatic Biological Microscope Objective Lens 40X	30
Light Source	White LED	1
Laser Source	Focusable, 12V, 600 mW, 405 nm CW laser module	100
OG515 filter	25.4 ×25.4 ×3 mm	29
Electrical components	N/A	20
3D-printed	PLA filament (1 kg)	20
	Total cost of proposed microscope	240

4. Discussion

Our initial hypothesis was that it was possible to build a low-cost fluorescence microscope by replacing the optical scheme of costly fluorescence filter cubes with a simplified filter system based on a laser and a cheap longpass barrier filter. Another hypothesis was that it was possible to reach enough magnification (of 400X) and use a smartphone to visualize fluorescence real biological samples for the diagnosis of diseases. Both of hypotheses were totally validated and confirmed with the obtained results.

We also demonstrated that our approach works, even though the low-cost laser source with 405 nm wavelength, is not the optimal one to reach the maximum of the 495 nm absorption peak of the FITC fluorophore. This opens the possibility of using other laser excitation sources with different wavelengths, closer to the peak of the fluorophore to be used. We also demonstrated this, during our validation with the calibration microbeads, by using two other fluorophores (PE and PE-Cy5) with different absorption peaks.

One of the key enabling ideas that makes our simplified filter system to correctly work, is its inverted optical scheme. Without the inverted scheme, it is not possible to have the excitation signal together with the fluorescence signal to reach the longpass filter, letting only the fluorescence signal to reach the smartphone's camera.

4.1. Advantages and disadvantages of our approach

We can summarize the advantages of our low-cost laser fluorescence inverted microscope as follows:

- The device is easily reproducible and affordable, just requiring a 3D-printer, a smartphone, and low-cost optical and mechanical components.

- The magnification of the device is at least 400X which is compatible with requirements for disease diagnosis (visualization of parasites and cells).
- The device works with FITC, the most commonly used fluorophore for disease diagnosis, but also works with other fluorophores.
- The use of a smartphone allows digital zoom to have a better visualization of the fluorescence images.
- The inverted optical scheme simplifies the positioning of the smartphone camera through the smartphone holder.
- The device is small, portable and does not require special working conditions.
- The X-Y and Z positioning system allows the microscope operator to handle the samples as in a conventional fluorescence microscope.

We can also mention some disadvantages of our approach, mainly related to the use of laser source:

- The use of a Class III laser module requires special care (e.g., using special protective eyewear) and operator training. We can mitigate this, by adding to the device a protection filter to absorb the laser excitation signal and by reducing the distance of the laser to the sample as much as possible.
- The exposure of the sample under laser radiation causes the fluorophores to degrade rapidly due to the high laser intensity (the fluorescence disappears after some seconds in our tests). This issue can be mitigated by enabling the intensity control system of the laser module (which works with a PWM pulse controller) which requires some electronic control system to be developed. Also, another possibility is to replace the laser module with another one, with a wavelength closer to the absorption peak of the fluorophore (e.g., a laser module with 488 nm wavelength for FITC). This option also requires a change on the longpass barrier filter, to reflect this change. This modification is totally valid but may increase the cost of the device.

4.2. Related work on low-cost fluorescence microscopy

The development of low-cost microscopes attracted a large body of researchers [27–32,42], thus giving an affordable alternative for developing countries, due to the high costs of conventional microscopes. In [48], more than 20 types of low-cost microscopes were analyzed and reviewed, where some of them use smartphones as their optical sensor. Furthermore, smartphone-based microscopy [26] has become an interesting alternative, enabling more compact, affordable, and flexible solutions compared to conventional microscopy.

Due to potential healthcare applications, such as detection and diagnosis of diseases, low-cost fluorescence microscopy was also developed in the recent years. Our work in grounded in previous work in fluorescence microscopy [32] and the development of a non-fluorescence inverted microscope [42]. In the first one, we used Rhodamine 6G dye both to filter the excitation signal of a laser at 532 nm and also to visualize the fluorescent particles of Rhodamine 6G. The microscope used a Raspberry Pi camera as optical sensor, and had only 100X of magnification. In the latter, the inverted non-fluorescence microscope used a smartphone to collect images and videos from the MODS technique (Microscopy Observation Drug Susceptibility) for tuberculosis diagnosis. The inverted optical scheme was important to allow Mycobacterium tuberculosis colonies grown in liquid media. We borrowed this inverted optical scheme, to simplify our laser-based filtering system. This microscope had only 100X of magnification, which was enough to identify large colonies of Mycobacterium tuberculosis cords in MODS cultures.

Table 2 gives an overview of related work on low-cost fluorescence microscopy. We can observe that only one fluorescence microscope (Miller et al. [33]) was applied to diagnosis of a disease. This is mainly due to the limited magnification of the other fluorescence microscopes, that do not reach the required 400X magnification, thus only allowing visualization of fluorescent biological and non-biological elements (e.g., cells, liver tissues, microbeads, and particles). Compared to our device, the microscope by Miller et al., also prevents the

Preprints (www.preprints.org) | NOT PEER-REVIEWED | Posted: 21 October 2022 doi:10.20944/preprints202210.0339.v1

use of fluorescence filter cube, by using an inverted scheme, but uses two filters (excitation filter and emission filter), uses spare parts of a conventional microscope, and does not use a smartphone.

The fluorescence microscope by Hasan et al. [31] is basically a re-implementation of a fluorescence filter cube, based on a low-cost commercial microscope with an integrated camera, a dichroic mirror, and two filters (excitation and barrier). This fluorescence microscope does not use a smartphone, requires a computer to operate, has only 200X, and does not have a positioning system.

Although, Schaefer et al. [34] proposed a fluorescence microscope with an automatized X-Y stage, similar to our previous work [32], the microscope focuses only on showing the feasibility of capturing fluorescent images as a proof-of-concept.

Dai et al. [29] proposes a fluorescence microscope, that uses a smartphone and a dual functional polymer for magnification and signal filtering, thus avoiding a costly fluorescence filter cube. The microscope uses different laser diodes as excitation source and has a resolution smaller than 200X, hence limiting its application only to visualization of tissues.

Zhu et al. [30] propose an smartphone-based inverted fluorescence microscope with 400X magnification that use an LED as excitation source, however it uses a fluorescence filter cube, making the price rise up to 3000 $.

Although, the microscopes by Kim et al. [27], Dai et al. [29], and Liu et al. [28], are all smartphone-based, they only use a magnification lens attached to the smartphone camera (instead of an objective and ocular lens), thus limiting the magnification (up to 200X) and making them unfeasible for disease diagnosis. In addition, they do not have any positioning stage.

Table 2. Related work on low-cost fluorescence microscopes

Authors, Reference, year	Smartphone based	Mag.	Emission source	Fluorophore	Type of application	Cost [USD]
Miller et al. [33] 2010	No	400X	Blue LED and excitation filter	Auramine	Diagnosis of M. tuberculosis	240-480
Schaefer et al. [34] 2012	No	200X	LED (460 nm)	N/A	Visualization of fluorescent microbeads	150
Kim et at. [27] 2015	Yes	200X	LED (405 nm) and Blue laser (445 nm)	Carboxyfluorescein succinimidyl	Visualization of cells	N/A
Hasan et al. [31] 2016	No	200X	Flashlight and excitation filter (380-500 nm)	Alexa Fluor 488	Visualization of cancer cells	358
Ormachea et al. [32] 2017	No	100X	Green laser (532 nm)	Rhodaimine 6G	Visualization of fluorescent particles	620
Dai et al. [29] 2019	Yes	<200X	Laser Diodes (365, 480, and 520 nm)	DAPI and Alex Fluor 488	Visualization of human liver tissues	N/A
Zhu et al. [30] 2020	Yes	400X	LED (470 nm)	PARPi-FL	Visualization of swine esophagus tissue cells	3000
Liu et al. [28] 2021	Yes	20X	UV LED (285 nm)	Rhodamine B DAPI and CytoStain	Visualization of mice live cells	20-50
Our device	Yes	400X	Blue Laser (405 nm)	FITC	Diagnosis of Chagas and ANCA	240

Overall, we can see that, compared to related work, our low-cost inverted fluorescence microscope fulfills the necessary features for real diagnosis of diseases and sample handling close to those used in commercial fluorescence microscopes.

5. Conclusions

We successfully designed, built, and tested a smartphone-based low-cost laser inverted fluorescence microscope for the diagnosis of diseases. Our device includes a simplified optical filter system (using a low-cost laser source and a cheap barrier filter), thus avoiding complex and costly filter system used in conventional fluorescence microscopes. We

validated our device with real biological samples of one infectious disease (Chagas) and one non-communicable disease (ANCA), both labeled with FITC fluorophore. This opens the possibility to apply our approach to any disease that uses FITC fluorophore for labeling. Our device has a 400X magnification and only costs 240 $. We believe that a low-cost fluorescence microscope can help on early diagnosis of diseases in countries with low-income settings, where the availability of conventional commercial fluorescence microscope is scarce or nonexistent.

Author Contributions: "Conceptualization, O.O. and M.Z.; methodology, O.O. and A.V.; software, A.V.; validation, O.O., P.R. and A.V.; investigation, O.O. and P.R.; resources, P.R.; writing—original draft preparation, O.O.; writing—review and editing, A.V. and O.O.; All authors have read and agreed to the published version of the manuscript."

Funding: This research received no external funding

Institutional Review Board Statement: Not applicable.

Acknowledgments: The authors would like to thank Amilcar Flores from Instituto de Investigaciones Biomédicas (IIBISMED), Facultad de Medicina, Universidad Mayor de San Simón (UMSS), for his valuable help in the preparation and labeling of the biological samples.

Conflicts of Interest: The authors declare no conflict of interest.

Sample Availability: Not applicable.

Abbreviations

The following abbreviations are used in this manuscript:

ANCA	Antineutrophil Cytoplasmic Antibodies
CW	Continuous Wave
FITC	Fluorescein Isothiocyanate
IFA	indirect immunofluorescent-antibody
LED	Light Emitting Diode
PLA	Polylactic Acid
PE	Phycoerythrin
PE-Cy5	Phycoerythrin - Cyanine 5
UV	Ultra Violet

References

25. Sanborn, W.R.; Heuck, C.; El Aouad, R.; Storch, W. *Fluorescence microscopy for disease diagnosis and environmental monitoring*; World Health Organization, Regional Office for the Eastern Mediterranean: Cairo, 2005. OCLC: 70225764.
26. Pfeil, J.; Dangelat, L.N.; Frohme, M.; Schulze, K. Smartphone based mobile microscopy for diagnostics. *Journal of Cellular Biotechnology* **2018**, *4*, 57–65. Publisher: IOS Press, https://doi.org/10.3233/JCB-180010.
27. Kim, J.H.; Joo, H.G.; Kim, T.H.; Ju, Y.G. A smartphone-based fluorescence microscope utilizing an external phone camera lens module. *BioChip Journal* **2015**, *9*, 285–292. https://doi.org/10.1007/s13206-015-9403-0.
28. Liu, Y.; Rollins, A.M.; Levenson, R.M.; Fereidouni, F.; Jenkins, M.W. Pocket MUSE: an affordable, versatile and high-performance fluorescence microscope using a smartphone. *Communications Biology* **2021**, *4*, 1–14. Number: 1 Publisher: Nature Publishing Group, https://doi.org/10.1038/s42003-021-01860-5.
29. Dai, B.; Jiao, Z.; Zheng, L.; Bachman, H.; Fu, Y.; Wan, X.; Zhang, Y.; Huang, Y.; Han, X.; Zhao, C.; et al. Colour compound lenses for a portable fluorescence microscope. *Light: Science & Applications* **2019**, *8*, 75. Number: 1 Publisher: Nature Publishing Group, https://doi.org/10.1038/s41377-019-0187-1.
30. Zhu, W.; Zhu, W.; Pirovano, G.; Pirovano, G.; O'Neal, P.K.; Gong, C.; Kulkarni, N.; Nguyen, C.D.; Brand, C.; Reiner, T.; et al. Smartphone epifluorescence microscopy for cellular imaging of fresh tissue in low-resource settings. *Biomedical Optics Express* **2020**, *11*, 89–98. Publisher: Optica Publishing Group, https://doi.org/10.1364/BOE.11.000089.
31. Hasan, M.M.; Alam, M.W.; Wahid, K.A.; Miah, S.; Lukong, K.E. A Low-Cost Digital Microscope with Real-Time Fluorescent Imaging Capability. *PLOS ONE* **2016**, *11*, e0167863. Publisher: Public Library of Science, https://doi.org/10.1371/journal.pone.0167863.
32. Ormachea, O.; Villazón, A. Development of a Low-Cost Epifluorescence Microscope. *Investigación & Desarrollo* **2017**, *1*, 5–14. https://doi.org/10.23881/idupbo.017.1-1i.

33. Miller, A.R.; Davis, G.L.; Oden, Z.M.; Razavi, M.R.; Fateh, A.; Ghazanfari, M.; Abdolrahimi, F.; Poorazar, S.; Sakhaie, F.; Olsen, R.J.; et al. Portable, Battery-Operated, Low-Cost, Bright Field and Fluorescence Microscope. *PLOS ONE* **2010**, *5*, e11890. https://doi.org/10.1371/journal.pone.0011890.
34. Schaefer, S.; Boehm, S.A.; Chau, K.J. Automated, portable, low-cost bright-field and fluorescence microscope with autofocus and autoscanning capabilities. *Applied Optics* **2012**, *51*, 2581–2588. https://doi.org/10.1364/AO.51.002581.
35. Antinori, S.; Galimberti, L.; Bianco, R.; Grande, R.; Galli, M.; Corbellino, M. Chagas disease in Europe: A review for the internist in the globalized world. *European Journal of Internal Medicine* **2017**, *43*, 6–15. https://doi.org/10.1016/j.ejim.2017.05.001.
36. Pareek, M.; Greenaway, C.; Noori, T.; Munoz, J.; Zenner, D. The impact of migration on tuberculosis epidemiology and control in high-income countries: a review. *BMC Medicine* **2016**, *14*, 48. https://doi.org/10.1186/s12916-016-0595-5.
37. Steingart, K.R.; Henry, M.; Ng, V.; Hopewell, P.C.; Ramsay, A.; Cunningham, J.; Urbanczik, R.; Perkins, M.; Aziz, M.A.; Pai, M. *Fluorescence versus conventional sputum smear microscopy for tuberculosis: a systematic review*; Centre for Reviews and Dissemination (UK), 2006. https://doi.org/10.1016/S1473-3099(06)70578-3.
38. Campos, Y.; Briceño, L.; Reina, K.; Figarella, K.; Pérez, J.L.; Mosca, W. Serological diagnosis of Chagas disease: evaluation and characterisation of a low cost antigen with high sensitivity and specificity. *Memórias do Instituto Oswaldo Cruz* **2009**, *104*, 914–917. https://doi.org/10.1590/S0074-02762009000600016.
39. Chandler, F.W.; Watts, J.C. Immunofluorescence as an adjunct to the histopathologic diagnosis of Chagas' disease. *Journal of Clinical Microbiology* **1988**, *26*, 567–569. https://doi.org/10.1128/jcm.26.3.567-569.1988.
40. The, T.H.; Feltkamp, T.E.W. Conjugation of fluorescein isothiocyanate to antibodies: I. Experiments on the conditions of conjugation. *Immunology* **1970**, *18*, 865. Publisher: Wiley-Blackwell.
41. Hagen, E.C.; Daha, M.R.; Hermans, J.; Andrassy, K.; Csernok, E.; Gaskin, G.; Lesavre, P.; Lüdemann, J.; Rasmussen, N.; Sinico, R.A.; et al. Diagnostic value of standardized assays for anti-neutrophil cytoplasmic antibodies in idiopathic systemic vasculitis. *Kidney International* **1998**, *53*, 743–753. https://doi.org/10.1046/j.1523-1755.1998.00807.x.
42. Salguedo, M.; Zarate, G.; Coronel, J.; Comina, G.; Gilman, R.H.; Sheen, P.; Oberhelman, R.; Zimic, M. Low-cost 3D-printed inverted microscope to detect Mycobacterium tuberculosis in a MODS culture. *Tuberculosis* **2022**, *132*, 102158. https://doi.org/10.1016/j.tube.2021.102158.
43. Schauenstein, K.; Schauenstein, E.; Wick, G. Fluorescence properties of free and protein bound fluorescein dyes. I. Macrospectrofluorometric measurements. *Journal of Histochemistry & Cytochemistry* **1978**, *26*, 277–283. https://doi.org/10.1177/26.4.77868.
44. Renshaw, S. Chapter 4.2 - Immunohistochemistry and Immunocytochemistry. In *The Immunoassay Handbook (Fourth Edition)*; Wild, D., Ed.; Elsevier: Oxford, 2013; pp. 357–377. https://doi.org/10.1016/B978-0-08-097037-0.00024-5.
45. Sjöback, R.; Nygren, J.; Kubista, M. Absorption and fluorescence properties of fluorescein. *Spectrochimica Acta Part A: Molecular and Biomolecular Spectroscopy* **1995**, *51*, L7–L21. https://doi.org/10.1016/0584-8539(95)01421-P.
46. McKay, I.C.; Forman, D.; White, R.G. A comparison of fluorescein isothiocyanate and lissamine rhodamine (RB 200) as labels for antibody in the fluorescent antibody technique. *Immunology* **1981**, *43*, 591. Publisher: Wiley-Blackwell.
47. Matsumoto, B., Ed. *Cell biological applications of confocal microscopy*, 2. ed., [nachdr.] ed.; Number 70 in Methods in cell biology, Academic Press: Amsterdam, 2004.
48. Salido, J.; Bueno, G.; Ruiz-Santaquiteria, J.; Cristobal, G. A review on low-cost microscopes for Open Science. *Microscopy Research and Technique* **2022**, pp. 1–14. Publisher: Wiley Analytical Science, https://doi.org/10.1002/jemt.24200.

References

25. Sanborn, W.R.; Heuck, C.; El Aouad, R.; Storch, W. *Fluorescence microscopy for disease diagnosis and environmental monitoring*; World Health Organization, Regional Office for the Eastern Mediterranean: Cairo, 2005. OCLC: 70225764.
26. Pfeil, J.; Dangelat, L.N.; Frohme, M.; Schulze, K. Smartphone based mobile microscopy for diagnostics. *Journal of Cellular Biotechnology* **2018**, *4*, 57–65. Publisher: IOS Press, https://doi.org/10.3233/JCB-180010.
27. Kim, J.H.; Joo, H.G.; Kim, T.H.; Ju, Y.G. A smartphone-based fluorescence microscope utilizing an external phone camera lens module. *BioChip Journal* **2015**, *9*, 285–292. https://doi.org/10.1007/s13206-015-9403-0.
28. Liu, Y.; Rollins, A.M.; Levenson, R.M.; Fereidouni, F.; Jenkins, M.W. Pocket MUSE: an affordable, versatile and high-performance fluorescence microscope using a smartphone. *Communications Biology* **2021**, *4*, 1–14. Number: 1 Publisher: Nature Publishing Group, https://doi.org/10.1038/s42003-021-01860-5.
29. Dai, B.; Jiao, Z.; Zheng, L.; Bachman, H.; Fu, Y.; Wan, X.; Zhang, Y.; Huang, Y.; Han, X.; Zhao, C.; et al. Colour compound lenses for a portable fluorescence microscope. *Light: Science & Applications* **2019**, *8*, 75. Number: 1 Publisher: Nature Publishing Group, https://doi.org/10.1038/s41377-019-0187-1.
30. Zhu, W.; Zhu, W.; Pirovano, G.; Pirovano, G.; O'Neal, P.K.; Gong, C.; Kulkarni, N.; Nguyen, C.D.; Brand, C.; Reiner, T.; et al. Smartphone epifluorescence microscopy for cellular imaging of fresh tissue in low-resource settings. *Biomedical Optics Express* **2020**, *11*, 89–98. Publisher: Optica Publishing Group, https://doi.org/10.1364/BOE.11.000089.
31. Hasan, M.M.; Alam, M.W.; Wahid, K.A.; Miah, S.; Lukong, K.E. A Low-Cost Digital Microscope with Real-Time Fluorescent Imaging Capability. *PLOS ONE* **2016**, *11*, e0167863. Publisher: Public Library of Science, https://doi.org/10.1371/journal.pone.0167863.
32. Ormachea, O.; Villazón, A. Development of a Low-Cost Epifluorescence Microscope. *Investigación & Desarrollo* **2017**, *1*, 5–14. https://doi.org/10.23881/idupbo.017.1-1i.

33. Miller, A.R.; Davis, G.L.; Oden, Z.M.; Razavi, M.R.; Fateh, A.; Ghazanfari, M.; Abdolrahimi, F.; Poorazar, S.; Sakhaie, F.; Olsen, R.J.; et al. Portable, Battery-Operated, Low-Cost, Bright Field and Fluorescence Microscope. *PLOS ONE* **2010**, *5*, e11890. https://doi.org/10.1371/journal.pone.0011890.
34. Schaefer, S.; Boehm, S.A.; Chau, K.J. Automated, portable, low-cost bright-field and fluorescence microscope with autofocus and autoscanning capabilities. *Applied Optics* **2012**, *51*, 2581–2588. https://doi.org/10.1364/AO.51.002581.
35. Antinori, S.; Galimberti, L.; Bianco, R.; Grande, R.; Galli, M.; Corbellino, M. Chagas disease in Europe: A review for the internist in the globalized world. *European Journal of Internal Medicine* **2017**, *43*, 6–15. https://doi.org/10.1016/j.ejim.2017.05.001.
36. Pareek, M.; Greenaway, C.; Noori, T.; Munoz, J.; Zenner, D. The impact of migration on tuberculosis epidemiology and control in high-income countries: a review. *BMC Medicine* **2016**, *14*, 48. https://doi.org/10.1186/s12916-016-0595-5.
37. Steingart, K.R.; Henry, M.; Ng, V.; Hopewell, P.C.; Ramsay, A.; Cunningham, J.; Urbanczik, R.; Perkins, M.; Aziz, M.A.; Pai, M. *Fluorescence versus conventional sputum smear microscopy for tuberculosis: a systematic review*; Centre for Reviews and Dissemination (UK), 2006. https://doi.org/10.1016/S1473-3099(06)70578-3.
38. Campos, Y.; Briceño, L.; Reina, K.; Figarella, K.; Pérez, J.L.; Mosca, W. Serological diagnosis of Chagas disease: evaluation and characterisation of a low cost antigen with high sensitivity and specificity. *Memórias do Instituto Oswaldo Cruz* **2009**, *104*, 914–917. https://doi.org/10.1590/S0074-02762009000600016.
39. Chandler, F.W.; Watts, J.C. Immunofluorescence as an adjunct to the histopathologic diagnosis of Chagas' disease. *Journal of Clinical Microbiology* **1988**, *26*, 567–569. https://doi.org/10.1128/jcm.26.3.567-569.1988.
40. The, T.H.; Feltkamp, T.E.W. Conjugation of fluorescein isothiocyanate to antibodies: I. Experiments on the conditions of conjugation. *Immunology* **1970**, *18*, 865. Publisher: Wiley-Blackwell.
41. Hagen, E.C.; Daha, M.R.; Hermans, J.; Andrassy, K.; Csernok, E.; Gaskin, G.; Lesavre, P.; Lüdemann, J.; Rasmussen, N.; Sinico, R.A.; et al. Diagnostic value of standardized assays for anti-neutrophil cytoplasmic antibodies in idiopathic systemic vasculitis. *Kidney International* **1998**, *53*, 743–753. https://doi.org/10.1046/j.1523-1755.1998.00807.x.
42. Salguedo, M.; Zarate, G.; Coronel, J.; Comina, G.; Gilman, R.H.; Sheen, P.; Oberhelman, R.; Zimic, M. Low-cost 3D-printed inverted microscope to detect Mycobacterium tuberculosis in a MODS culture. *Tuberculosis* **2022**, *132*, 102158. https://doi.org/10.1016/j.tube.2021.102158.
43. Schauenstein, K.; Schauenstein, E.; Wick, G. Fluorescence properties of free and protein bound fluorescein dyes. I. Macrospectrofluorometric measurements. *Journal of Histochemistry & Cytochemistry* **1978**, *26*, 277–283. https://doi.org/10.1177/26.4.77868.
44. Renshaw, S. Chapter 4.2 - Immunohistochemistry and Immunocytochemistry. In *The Immunoassay Handbook (Fourth Edition)*; Wild, D., Ed.; Elsevier: Oxford, 2013; pp. 357–377. https://doi.org/10.1016/B978-0-08-097037-0.00024-5.
45. Sjöback, R.; Nygren, J.; Kubista, M. Absorption and fluorescence properties of fluorescein. *Spectrochimica Acta Part A: Molecular and Biomolecular Spectroscopy* **1995**, *51*, L7–L21. https://doi.org/10.1016/0584-8539(95)01421-P.
46. McKay, I.C.; Forman, D.; White, R.G. A comparison of fluorescein isothiocyanate and lissamine rhodamine (RB 200) as labels for antibody in the fluorescent antibody technique. *Immunology* **1981**, *43*, 591. Publisher: Wiley-Blackwell.
47. Matsumoto, B., Ed. *Cell biological applications of confocal microscopy*, 2. ed., [nachdr.] ed.; Number 70 in Methods in cell biology, Academic Press: Amsterdam, 2004.
48. Salido, J.; Bueno, G.; Ruiz-Santaquiteria, J.; Cristobal, G. A review on low-cost microscopes for Open Science. *Microscopy Research and Technique* **2022**, pp. 1–14. Publisher: Wiley Analytical Science, https://doi.org/10.1002/jemt.24200.